JOURNAL OF COMPUTATIONAL PHYSICS **131,** 253–266 (1997)
ARTICLE NO. CP965614

Bifurcation Analysis of Brown Tide by Reaction–Diffusion Equation Using Finite Element Method

Mutsuto Kawahara and Yan Ding

Department of Civil Engineering, Chuo University, Kasuga 1-13-27, Bunkyo-ku, Tokyo 112, Japan
E-mail: ding@indy2.civil.chuo-u.ac.jp.

Received January 22, 1996; revised September 30, 1996

In this paper, we analyze the bifurcation of a biodynamics system in a two-dimensional domain by virtue of reaction–diffusion equations. The discretization method in space is the finite element method. The computational algorithm for an eigenspectrum is described in detail. On the basis of an analysis of eigenspectra according to Helmholtz's equation, the discrete spectra in regards to the physical variables are numerically obtained in two-dimensional space. In order to investigate this mathematical model in regards to its practical use, we analysed the stability of two cases, i.e., hydranth regeneration in the marine hydroid *Tubularia* and a brown tide in a harbor in Japan. By evaluating the stability according to the linearized stability definition, the critical parameters for outbreaks of brown tide can be theoretically determined. In addition, results for the linear combination of eigenspectrum coincide with the distribution of the observed brown tide. Its periodic characteristic was also verified.

I. INTRODUCTION

A reaction–diffusion system can be represented by the following equations [1, 2]

$$\dot{\mathbf{u}} = \mathbf{F}(\lambda, \mathbf{u}) + D\nabla^2\mathbf{u}, \tag{1}$$

where $\mathbf{u}$ is in a Hilbert space, generally, and denotes a vector describing the density of certain substances. The dot represents the derivative with respect to time and is the rate of a change in species in the brown tide. $\mathbf{F}$ is an operator and denotes the rate of species reaction in the brown tide, e.g., the growth rate or dissipation–production term. ∇^2 is the Laplacian operator. The third term in (1) indicates the effect of diffusion, which may represent molecular diffusion or the random movement of individuals in a population. Furthermore, D represents a diffusion matrix. Parameter λ is referred to as a bifurcation parameter which we shall assume to be scalar for simplicity (e.g., $\lambda > 0$). See Aris [1] for an application of a similar equation to chemical reaction theory, and Murray [6] for an application to a biological system.

In general, Hilbert space will normally be completed under a norm that is derived from a suitable inner product of function space $\mathbf{u}(\mathbf{r}, t)$ as defined on domain $Q = \Omega \times (-\infty, +\infty)$, where $\Omega \subset R^n$ (which are sufficiently smooth for the relevant derivatives to be continuous and such that the correct boundary conditions are satisfied). The equilibrium solutions of evolution equations (1) that are subject to specified boundary conditions may be steady, periodic, or other forms. It is necessary to consider the stability of the solution since an unstable equlibrium solution for equations is not physical.

The finite element method has enabled the linear-elastic instability analysis of practical structures under complex load conditions [9]. The critical feature of the discrete system for a buckling load can be obtained under linearized stability by a finite element method. Apart from the influence of nonlinear reaction terms in a reaction–diffusion system, the diffusion matrix has the same function as the stiffness one in structural analysis. Spectra are similar to the normal modes of a structure from the generalized eigenproblem [10]. It has been proven that the Ritz–Galerkin method is advantageous in regards to accuracy, efficiency, and ability to approach the complex geometries in question.

As one of the most important environmental problems in oceanic ecology, the generation rate of phytoplankton in a brown tide can be represented by a reaction process, such as the Lotka–Volterra system and other prey–predator systems [3]. Although all of the above systems are simply expressed as two ordinary differential equations, they reveal the mechanism about the population oscillation. If we further consider the effect of diffusion and even convection under a reaction–diffusion system, along with an increase of the physical processes in the mathematical model, bifurcation parameter λ in the onset of a brown tide can be determined under the definition of linearized stability [3]. The parameter can explain the outbreak of brown tides from a bifurcation point of view. In a linearized system, the regular pattern in a practical field that is seen during this development may be the result of a combination of the spectra of the reaction–diffusion system. To produce such patterns, a

0021-9991/97 $25.00

reaction–diffusion system would have to have a steady state that is stable to spatially homogeneous perturbation but unstable to spatially inhomogeneous ones (or at least more unstable to inhomogeneous than to homogeneous perturbation).

In this paper, we will first consider hydranth regeneration in the marine hydroid *Tubularia* in a regular geometrical boundary with spatially homogeneous perturbation. This proves that the result obtained with *Tubularia* is in agreement with that in observation [2]. Then, we will focus on the brown tide at Maizuru Harbor near the sea of Japan [7] and will utilize the reaction–diffusion equations as a mathematical model in regards to the evolution of phytoplankton in brown tides. Moreover, we have used spectrum analysis (of spatially inhomogeneous perturbation) in regards to a distribution of plankton based on the solution of Helmholtz's equation with the finite element method. These spectra are similar to the normal modes that result from a freely vibrating undamped system in structural analysis. The stability concept is used in order to judge the unstable and asymptotically stable. Outbreak parameter λ can also be obtained and certain linear combination patterns in the spectrum are compared with observation data. They are in very close agreement.

The remainder of the paper is organized as follows. Sections 2 describes the partial differential equations of the system. In Section 3, the implementation aspects of stability are discussed by means of the finite element method. In Section 4, the eigenspectrum solvers and algorithms in both symmetrical and unsymmetrical matrices are described for the generalized eigenproblem. The determination of the parameters and the discretization of computational domain are discussed in Section 5. The results of the stability and the bifurcation properties of *Tubularia* and the brown tide are analysed in Section 6 in detail. Section 7 concludes the paper.

2. SYSTEM MODEL

For the reaction–diffusion system, a set of two-component equations are used, as shown in Eqs. (2)

$$\dot{u} = \lambda f(u, v) + D_1 \nabla^2 u, \quad \dot{v} = \lambda g(u, v) + D_2 \nabla^2 v, \quad (2)$$

where u and v denote the density of certain substances. D_1 and D_2 are the unequal diffusivity of two kinds of species. Functions f and g are given as

$$f(u, v) = J_1 - u - \rho h(u, v) \quad (3)$$

$$g(u, v) = \alpha(J_1 - v) - \rho h(u, v) \quad (4)$$

$$h(u, v) = \frac{uv}{1 + u + Cu^2}, \quad (5)$$

where f and g have continuous second-order spatial and first-order temporal derivatives. The constants $D_1, D_2, J_1, J_2, \alpha, \rho, C$ are considered to be fixed. If domain Ω is defined in a two-dimensional plane, and $\mathbf{n}$ is defined as the unit outward normal vector, the boundary condition of species flux is imposed as

$$\nabla u \cdot \mathbf{n} = \nabla v \cdot \mathbf{n} = 0 \quad \text{on boundary } \Gamma. \quad (6)$$

3. STABILITY ANALYSIS

In this section, we will discuss linearized stability in the reaction–diffusion system by employing an approximation of the finite element method. To search for a spatial nonuniform structure in bounded domains with zero-flux boundary conditions (this kind of spatial heterogeneity in ecology is known as *patchiness* [6]), the eigenspectrum of the operator $-\nabla^2$ is introduced in order to analyze the linear stability of the discrete spectrum according to the finite element method. The stability of the spatial structure is judged in terms of the definition of linearized stability by Kielhöfer [4].

3.1. Finite Element Analysis (Eigenvalue Method)

The stability of the trivial solution for a nonlinear system (2) is often determined by the corresponding linearized system, i.e.,

$$\dot{\mathbf{v}} = \lambda M \mathbf{v} + D \nabla^2 \mathbf{v}, \quad (7)$$

where M denotes the Jacobian matrix, i.e.,

$$M = \begin{bmatrix} f_{,u} & f_{,v} \\ g_{,u} & g_{,v} \end{bmatrix}, \quad D = \begin{bmatrix} D_1 & \\ & D_2 \end{bmatrix}. \quad (8)$$

The matrix form of (7) can be rewritten as

$$\begin{bmatrix} \dot{u} \\ \dot{v} \end{bmatrix} = \lambda \begin{bmatrix} f_{,u} & f_{,v} \\ g_{,u} & g_{,v} \end{bmatrix} \begin{bmatrix} u \\ v \end{bmatrix} + \begin{bmatrix} D_1 \nabla^2 u & \\ & D_2 \nabla^2 v \end{bmatrix}. \quad (9)$$

Considering the zero-flux boundary condition (6), the discretization of finite element for (9) in subspace becomes

$$\begin{bmatrix} S^e & \\ & S^e \end{bmatrix} \begin{bmatrix} \dot{u}^e \\ \dot{v}^e \end{bmatrix} = \left\{ \lambda \begin{bmatrix} f^e_{,u} S^e & f^e_{,v} S^e \\ g^e_{,u} S^e & g^e_{,v} S^e \end{bmatrix} - \begin{bmatrix} D_1 K^e & \\ & D_2 K^e \end{bmatrix} \right\} \begin{bmatrix} u^e \\ v^e \end{bmatrix}, \quad (10)$$

where superscript e denotes the variable defined in the element. Given interpolation function ϕ, elemental matrices S^e and K^e are shown as

$$S^e = \int_{v^e} \phi_\alpha \phi_\beta dv^e, \quad K^e = \int_{v^e} \phi_{\alpha,i} \phi_{\beta,i} dv^e, \tag{11}$$

where α and β indicate the interpolation function index and i is that of spatial dimensions, respectively. Provided

$$\mathbf{v} = \Phi e^{\sigma t}, \tag{12}$$

then, (10) can be represented in the form

$$\sigma B \Phi = A \Phi, \tag{13}$$

where σ and Φ denote the eigenvalue and eigenvector of the linearized system (7), respectively. Meanwhile, elemental matrices A^e and B^e can be shown as

$$A^e = \begin{bmatrix} \lambda f^e_{,u} S^e - D_1 K^e & \lambda f^e_{,v} S^e \\ \lambda g^e_{,u} S^e & \lambda g_{,v} S^e - D_2 K^e \end{bmatrix}$$
$$B^e = \begin{bmatrix} S^e & \\ & S^e \end{bmatrix}. \tag{14}$$

In general, matrix A is nonsymmetric. So the set of σ is the set of complex numbers. For the case of a system of reaction–diffusion equations defined on a bounded spatial domain, the spectrum consists entirely of eigenvalues. According to the principle of linearized stability from Kielhöfer [4], if spectrum $\sigma(\lambda)$ is contained in the left-half plane and bounded away from the imaginary axis, the trivial solution of (2) is asymptotically stable. If $\sigma(\lambda)$ contains a point in the right open half plane at least, the trivial solution is unstable. Thus, for a system on a bounded spatial domain, we merely have to check that all eigenvalues $\sigma(\lambda)$ are in the left-half complex plane for asymptotic stability, and only if $\sigma(\lambda)$ contains a point in the right plane is the trivial solution of Eq. (2) unstable.

3.2. Spectra Analysis

As to the nonlinear system (2), we refer to the linearized operator $L(\lambda)$ as

$$L(\lambda) = \lambda M + D\nabla^2. \tag{15}$$

Thus, the eigenspectra of this linearized system in the infinite dimension are shown as

$$L\Phi = \sigma\Phi. \tag{16}$$

If the eigenvalues of operator $-\nabla^2$ on the domain Ω with the given boundary condition (6) are given by ω^2, then spectral problem (16) has a trivial solution or is given by

$$\det(\sigma I - L) = \begin{vmatrix} \sigma + D_1\omega^2 - \lambda f_{,u} & -\lambda f_{,v} \\ -\lambda g_{,u} & \sigma + D_2\omega^2 - \lambda g_{,v} \end{vmatrix}, \tag{17}$$

where I is the identity. To find the possible values which ω^2 may take we must solve the Helmholtz equation [8], i.e.,

$$\nabla^2 u + \omega^2 u = 0 \quad \text{in } \Omega. \tag{18}$$

If there are nontrivial solutions in Eq. (16), by keeping the polynomial (17) as zero, the eigenvalues $\sigma_n(\lambda)$ of $L(\lambda)$ are given by the roots of

$$\sigma_n^2 + [(D_1 + D_2)\omega_n^2 - \lambda \operatorname{tr} M]\sigma_n + Q_n(\lambda) = 0, \tag{19}$$

where

$$Q_n(\lambda) = \lambda^2 \det M - \lambda\omega_n^2(D_2 f_{,u} + D_1 g_{,v}) + D_1 D_2 \omega_n^4 \tag{20}$$

and the trace and determinant of M are

$$\operatorname{tr} M = f_{,u} + g_{,v}, \quad \det M = f_{,u} g_{,v} - f_{,v} g_{,u}. \tag{21}$$

Routh–Hurwitz's criterion states that both the roots σ_n of (19) have negative real parts if and only if

$$(D_1 + D_2)\omega_n^2 - \lambda \operatorname{tr} M > 0, \quad Q_n(\lambda) > 0. \tag{22}$$

Then, all of eigenvalues $\sigma(\lambda)$ are located on the left-half plane, and the solution of $\mathbf{u}$ is asymptotically stable.

3.3. Substitution Method

The finite element approximation of Helmholtz's equation (18) can be derived in subspace as

$$Ku = \omega^2 Su. \tag{23}$$

When the stability of the spectrum is checked by means of the finite element analysis, i.e., eigenvalue method, the formulation (23) can be directly substituted into (10), Eq. (13) can be reduced as

$$\sigma B \Phi = \acute{A} \Phi, \tag{24}$$

where elemental matrix $\acute{A}^e$ can be written as

$$\acute{A}^e = \begin{bmatrix} (\lambda f^e_{,u} - D_1\omega^2)S^e & f^e_{,v}S^e \\ \lambda g^e_{,u}S^e & (\lambda g^e_{,v} - D_2\omega^2)S^e \end{bmatrix}. \quad (25)$$

Generally, matrix $\acute{A}$ is nonsymmetric. Actually this stability analysis is the modified version of the finite element analysis as described above.

4. EIGENSPECTRUM SOLUTION

With respect to the stability analysis as stated above, there are three kinds of methods to check the stability in the eigenspectrum. In the computation of finite element equations in the eigenvalue problems, there actually are two types of equations in the generalized eigenspectrum problem, i.e., those of the symmetrical matrix and the nonsymmetrical matrix in Eqs. (13) and (24). The general formulation of an eigenspectrum in the above section can be written as

$$A\Phi = \sigma B\Phi. \quad (26)$$

Before the calculation of the spectrum in (26), the transformation is necessary in order to obtain the standard eigenvalue problem [5].

First, because of the symmetry in matrix B, this matrix can be factorized into an upper triangular matrix and into a lower one by Cholesky factorization, i.e.,

$$B = L^T L. \quad (27)$$

Setting vector $z = L\Phi$, we substitute these formulae into Eq. (26) and we get

$$A\Phi = \sigma L^T L\Phi. \quad (28)$$

Multiplying the equation as shown above by L^{-T}, then

$$L^{-T}AL^{-1}z = \sigma z. \quad (29)$$

If a matrix

$$H = L^{-T}AL^{-1}, \quad (30)$$

one can transfer Eq. (26) into the form

$$Hz = \sigma z. \quad (31)$$

In general, the eigenvalue problem of Eq. (26) is equivalent to the eigenvalue solution for matrix H, as in

$$\begin{aligned} L^{-T}AL^{-1}z &= \sigma z \\ \Rightarrow L^{-T}(A - \sigma L^T L)L^{-1}z &= 0 \\ \Rightarrow L^{-T}(A - \sigma B)L^{-1}z &= 0. \end{aligned} \quad (32)$$

Then, the eigenvectors Φ can be computed from the equation $\Phi = L^{-T}z$, by using backward substitution for the upper/lower triangle matrix. In the practical calculation of (31), if A is symmetrical and matrix H still keeps a symmetrical feature through the transformation, we can adopt some calculation algorithm in order to obtain an accurate spectrum, as stated in the following. However, if it is nonsymmetrical, the QR method is effective in order to get the eigenvalues in the system (31).

4.1. Computation of Spectra for Symmetrical Matrix

In eigenspectrum computation for the Helmholtz equation, matrix A is symmetrical. In addition, we are only concerned with a small number of eigenvalues and eigenvectors in the practical field, so the above-mentioned computational method can be modified and accelerated by the Strum bisection method and subspace iteration and inverse interaction, according to the computational sequence of successive increase or decrease in eigenvalues. The procedure for the calculation of the spectrum in the Helmholtz equation (for symmetrical A) is listed as follows:

Step. 0. (Start) Assumption of initial data

Step. 1. Automatic mesh generation

Step. 2. Check the mesh and half bandwidth for each element

Step. 3. Calculation of matrices A and B

Step. 4. Calculation of eigenvalues and eigenfunctions

Step. 4.1. Computation of matrix norm

Step. 4.2. Generalized Strum calculation for the symmetric band matrix from the smallest eigenvalue to the largest by means of Martin-Wilkinson's special Gaussian elimination

Step. 4.3. Bisection

Step. 4.4. Subspace iteration for symmetric band matrix

Step. 4.5. Analysis of error

Step. 5. Evaluation of stability for a system under the definition of the linearized stability

Step. 6. Output of results and graph

4.2. Computation of Spectra for Nonsymmetrical Matrix

Because of nonsymmetry in matrix A, it is effective for the calculation of the spectrum in Eqs. (13) and (24) by using the QR method, since a complex eigenvalue exists

in this case. The algorithm of this case for nonsymmetrical matrix A can be shown as follows:

Step. 0. (Start) Calculation of matrices A and B

Step. 1. Factorization of matrix B by using the Cholesky factorization

Step. 2. Calculation of matrix H

Step. 3. Calculation of the upper Hessenberg matrix of H by using the Householder reduction

Step. 4. Calculation of the eigenvalues σ by means of the QR method

Step. 5. If the calculation of eigenvector Φ is needed, then go to

Step. 5.1. Calculation of eigenvector z by using inverse iterative method

Step. 5.2. Calculation of eigenvector Φ by means of the backward substitution

Step. 6. Stop

5. DETERMINATION OF PARAMETERS AND DISCRETIZATION OF COMPUTATIONAL DOMAIN

5.1. Case 1

In the first case, the hydranth regeneration in the marine hydroid *Tubularia* is analysed. The considered domain is defined in a hollow cylinder, i.e., $\Omega = \{(r, \theta)|_{1<r<\delta,\ 0\le\theta<2\pi}\}$. δ is the nondimensional outer radius r_2 of the cylinder, i.e., $\delta = r_2/r_1$, in which r_1 denotes the inner radius. The boundary condition is that of zero-flux in the inner and outer circumferences. Given the scales of the physical variables u_0, T_0, and L_0 which denote the maximum concentration of pigment in the *Tubularia,* the scale of time and the inner radius, respectively, nondimensional equations (2) can be rewritten as

$$\frac{\partial u^*}{\partial t^*} = \lambda f(u^*, v^*) + D_1^* \nabla^2 u^* \tag{33}$$

$$\frac{\partial v^*}{\partial t^*} = \lambda g(u^*, v^*) + D_2^* \nabla^2 v^*, \tag{34}$$

where the asterisk indicates the nondimensional meaning. Thus, the nondimensional diffusion coefficient can be shown as $D_1^* = D_1 T_0 / L_0^2$. In this case, we have chosen diffusivity D_1^* as the unity for simplicity. Diffusion D_2^* can be referred to as the half of the value of D_1^*.

The computation domain in this hollow cylinder can be divided into triangular subspaces. The circumference is divided equally into a series of gaps and the polar gaps are also equally spaced. There are 400 nodes and 700 elements for the system of mesh when $\delta = 1.2$ and 1.5.

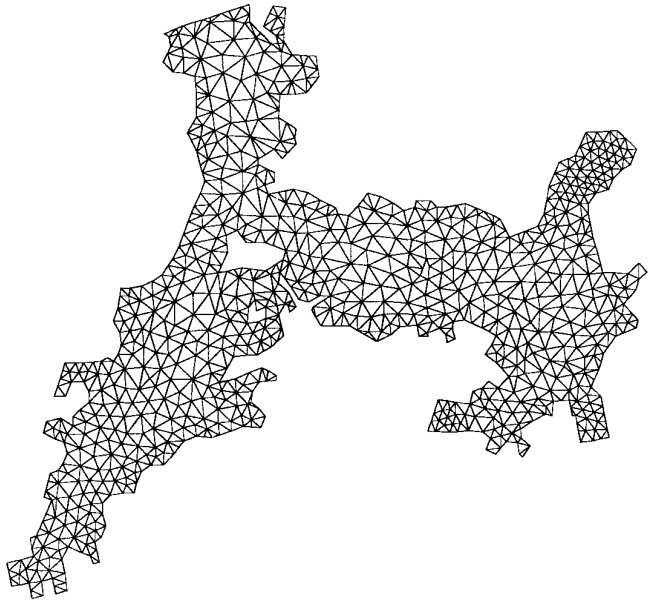

FIG. 1. Mesh in Maizuru Harbor.

5.2. Case 2

As for the reaction–diffusion system for two of the phases of the species in Maizuru Harbor, variable u denotes the density of a microalga in a cell per liter at time t, and v is the density of all other competing phytoplankton species in the same coastal waters. The scales of physical variables u_0, T_0, and L_0 denote the maximum density of phytoplankton, the period of pigment change from the bright to the dark patch in the brown tide, and the maximum averaged length of a patch, respectively. According to the field data on Sept. 17–23, 1978, in Maizuru Harbor, the above-mentioned scale parameters can be chosen as $T_0 = 2.5$ h and $L_0 = 1000.0$ m. As the diffusion observed is approximately 0.175 m^2/s (see [7]), we can deduce that the value of the nondimensional diffusion coefficient is $D_1^* = 1.26 \times 10^{-3}$. Generally, diffusion D_2^* can be referred to as half of D_1^*. The discretization of the computational domain is presented in Fig. 1. The mesh is generated automatically in which the discrete element system is 1446 and the total number of nodal points is 926.

6. RESULTS AND ANALYSIS

6.1. *Tubularia*

The eigenspectrum of the Helmholtz equation (18) (that is, the spectrum of linearized system (2) in a hollow cylinder) can be solved by employing the computational algorithm on the symmetrical matrix as stated above from the smallest eigenvalue to the largest one. As the number of eigenvalues is the same as the total degrees of freedom of the discrete system, for simplicity only the first 20 eigen-

TABLE I

Eigenvalues and Residual Error in Tubularia

No.	ω^2	ε
1	0.2953246123D-14	0.2082257100D-12
2	0.6526687327D+00	0.1337463674D-13
3	0.6526687327D+00	0.1464872416D-13
4	0.2612193613D+01	0.3627445799D-13
5	0.2612193613D+01	0.1709485532D-13
6	0.5883799667D+01	0.2311083116D-13
7	0.5883799667D+01	0.2831008046D-13
8	0.1047847286D+02	0.4069199367D-13
9	0.1047847286D+02	0.2531656051D-13
10	0.1641642779D+02	0.2278095144D-13
11	0.1641642779D+02	0.2225106284D-13
12	0.5883799667D+01	0.2875368709D-12
13	0.5883799667D+01	0.7127917364D-12
14	0.2612193613D+01	0.3890947212D-11
15	0.2612193613D+01	0.6711484956D-12
16	0.6526687327D+00	0.3732418061D-11
17	0.6526687327D+00	0.8704263516D-12
18	0.6950272065D-14	0.1403421447D-11
19	0.2373172252D+02	0.1179404502D-11
20	0.2373172252D+02	0.3603360401D-12

values are listed in Table I in which $\delta = 1.5$. Moreover, the residual error of the corresponding eigenvalue can be defined as

$$\varepsilon = \frac{\|Au - \omega^2 Bu\|_2}{\|Au\|_2}, \tag{35}$$

where $\|\cdot\|_2$ denotes the 2-norm of a vector and the eigenvalue is represented by ω^2 as the result of symmetrical positive matrices A and B in the Helmholtz equation (18). The eigenvalues occur in pairs, the most algebraic multiplicity being $m_i = 2$ (except for the first and 18th eigenvalues). The patterns of the corresponding eigenvalues are symmetrical with the origin of a hollow cycle (see Fig. 2.1). It means that the eigenfunction solution is a spatially homogenous perturbation.

According to the definition of stability for the linearized system, the stability of this reaction–diffusion system is analyzed. First, we will show the distribution of eigenfunctions in the ring in Figs. 2.1(2)a–d for $\delta = 1.2$ and $\delta = 1.5$, respectively. The dark regions represent areas where u is positive and the light regions where it is negative. In addition, the results obtained by means of a linearized analytical method are compared with those from a nonlinear finite element method for reaction–diffusion system (2) [3]. If division number NT (i.e., the wave number of the eigenfunction) in the circumference is small, the present results are similar to those obtained by using the nonlinear analysis method with FEM. However, when $\omega^2 \geq 6.3874$, the patterns of distribution for eigenvectors have a secondary division in the polar direction, when ω is a simple eigenvalue of the spectrum, i.e., $m_i = 1$. This means the so-called secondary bifurcation. The larger the eigenvalue is, the more patches occur in the hollow domain. According to observations in experiment [3], the pigment (i.e., concentration) represents the strength of hydranth regeneration in *Tubularia.* It follows that the eigenvectors obtained are very close to the distribution of pigment in reality when λ

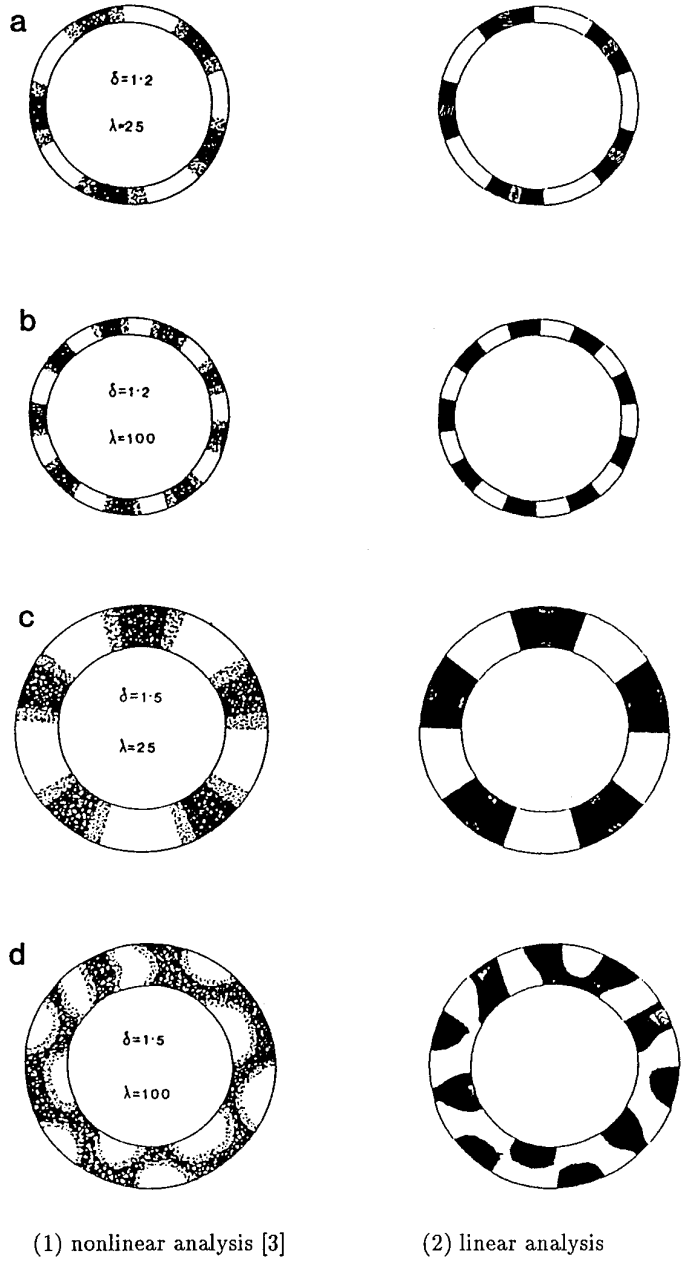

FIG. 2.1. Comparison of results obtained from nonlinear and linear analysis.

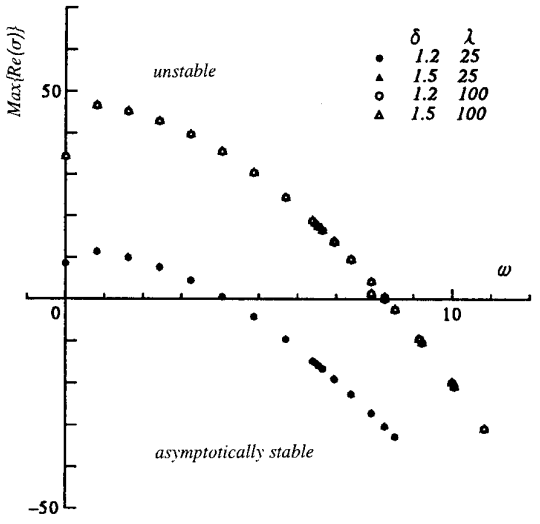

FIG. 2.2. Maximum real part of $\sigma(\lambda) \sim \omega$.

is small. Meanwhile, since the distribution of pigment in Fig. 2.1(1)d can be considered as a composite which consists of the modes of No. 25 (*double bifurcation point*), 40 ($NT = 10$) and 44 ($NT = 11$), we can add up the above three modes and show the results in Fig. 2.1(2)d. It shows that the result for a linearized system is very close to that of a nonlinear one when the so-called secondary bifurcation happens in the smaller λ.

By using the spectra analysis method, we can search for the most unstable point for each of the parameters (δ and λ), so long as one compares the maximum real part of $\sigma(\lambda)$ with the others (see Fig. 2.2). For example, the upper half of the plane denotes the unstable regime as there is at least one eigenvalue which extends to the right half of the plane. The most unstable point exists in each case for parameters δ and λ, and the stability has a closer dependence on parameter λ but not on δ.

6.2. Brown Tide

In this section, we will discuss four aspects in regards to stability in the brown tide at Maizuru Harbor: a solution for the Helmholtz equation by using the finite element method, a comparison amongst the three kinds of methods for stability analysis as described above, analysis of bifurcation parameter λ in the reaction–diffusion system, and a solution for the brown tide, based on the linear combination.

6.2.1. *Solution for a Helmholtz Equation*

By employing the computational algorithm in regards to the symmetrical matrix just as for the spectrum solution in *Tubularia,* we can obtain a spectrum for the linearized system in this brown tide from Helmholtz's equation as stated above. As a result, only the first 20 eigenvalues are listed in Table II. The eigenvalues occur in a simplex, i.e., algebraic multiplicity $m_i = 1$, compared with those in *Tubularia,* because there is not a geometrically symmetrical origin within the computational domain. The eigenvector patterns for the eigenvalue numbers 2–5 listed in Table II are shown in Figs. 3a–d. In these patterns, the density isolines denote that the density is positive; inversely, the white region denotes that the density is negative. It is obvious that the patch of brown tide oscillates in two-dimensional space. The more ω increases, the larger the number of the patch is. Eigenvalue ω can be considered as a frequency parameter in regards to density perturbation. The Helmholtz equation can also represent the perturbation of water height in shallow water so we can consider that the frequency of the transportation of the patch is consistent with that of water wave travel. This was proven from the angle of observation [7].

6.2.2. *Comparison of Results in Regards to Spectrum Stability*

In order to compare the spectrum as regards the stability in the reaction diffusion system from the three different methods mentioned above, we considered the parameter $\delta = 1.5$ and $\lambda = 25$ for *Tubularia,* and $\lambda = 1.5 \times 10^{-3}$ for the brown tide, as shown in Figs. 4a and b, respectively. With respect to the spectra analysis (local analysis method) and the substitution method, it is the same for the stability result by checking the maximum real part of the eigenvalue

TABLE II

Eigenvalues and Residual Error in Brown Tide

No.	Eigenvalue	ε
1	0.3156154301D-15	0.3035464564D-10
2	0.6300295891D-01	0.3285988889D-10
3	0.1420206070D+00	0.1041211708D-11
4	0.4077687592D+00	0.1127543462D-11
5	0.5505448178D+00	0.9889151215D-10
6	0.5772813529D+00	0.1133638092D-09
7	0.1132876394D+01	0.5679208651D-10
8	0.1336440419D+01	0.6632475055D-10
9	0.1732569259D+01	0.2305989155D-10
10	0.2052574221D+01	0.1074617023D-12
11	0.2137504154D+01	0.2596854856D-11
12	0.2540314010D+01	0.8511505946D-12
13	0.2916519498D+01	0.1318674609D-09
14	0.2959111655D+01	0.1256005206D-09
15	0.3422775077D+01	0.4157083980D-12
16	0.3656839971D+01	0.8795145548D-10
17	0.3900551695D+01	0.7849843760D-10
18	0.4372241801D+01	0.9087895776D-10
19	0.4457264717D+01	0.8366920249D-10
20	0.4891238593D+01	0.2382478649D-10

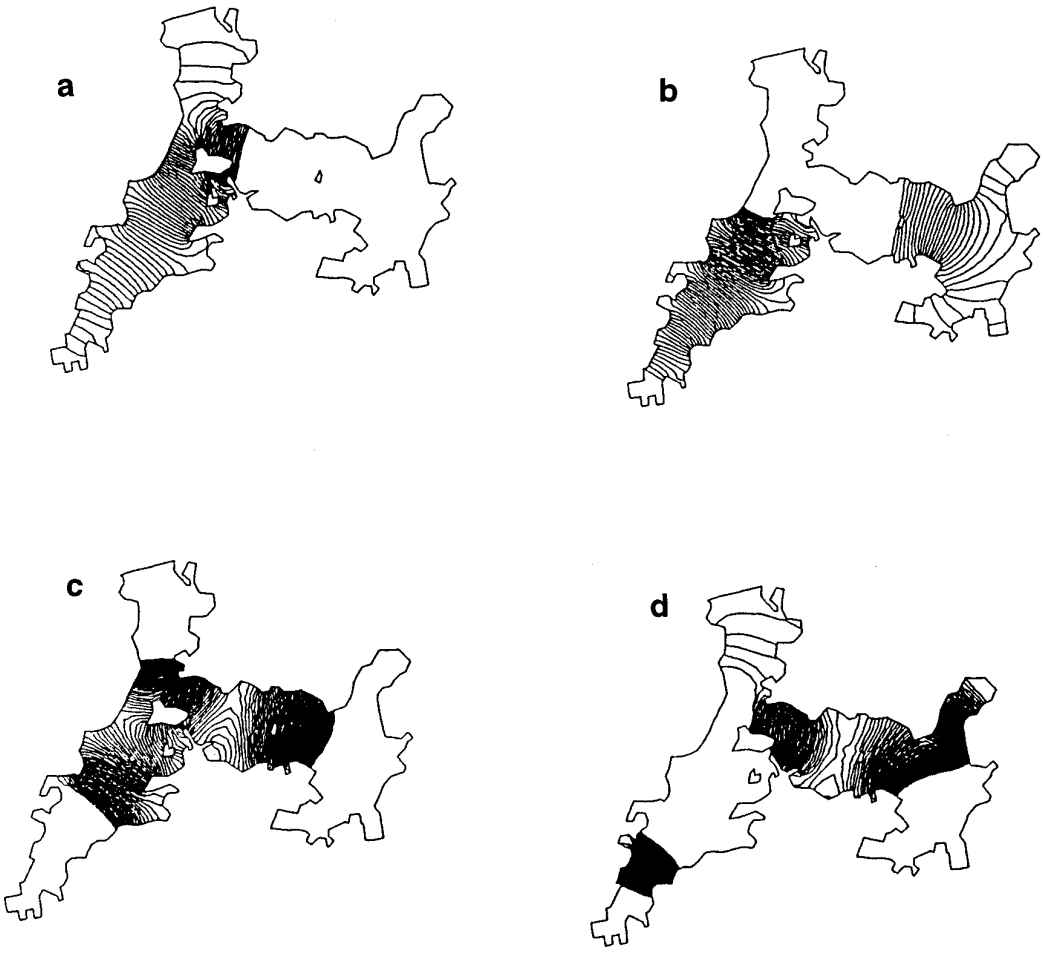

FIG. 3. Distribution of eigenvectors in brown tide.

$\sigma(\lambda)$, since Eq. (24) includes the characteristics of the wave oscillation in terms of the substitution of (23) into (10). However, the stability result from the eigenvalue method (global analysis method) is different as regards the results obtained by the two methods stated above. It results from matrix K in (10); that is, this matrix does not entirely represent the oscillation feature in the conventional linear interpolation of a triangular element. Along with an increase in wave number ω, this difference will become quite a bit larger. Thus it implies that the spectra analysis method and the substitution method are better than the eigenvalue method.

6.2.3. *Analysis of Bifurcation Parameter* λ

By using the spectra analysis method and checking spectrum stability under many kinds of parameter λ, in Fig. 5 we show a bifurcation diagram between ω and λ in the brown tide. The shaded region is the unstable area, the white is asymptotically stable, and the dark point denotes the results of stability analysis. The development of this reaction–diffusion advances gradually. First, the patterns with the lowest frequency become unstable and the corresponding critical point $(\lambda_{01}, \omega_{01})$ is singular in a $\lambda - \omega$ plane. The system in the left side of this point is asymptotically stable. Then, when the patterns with the lower frequency are converted to unstable, the second singular point is $(\lambda_{02}, \omega_{02})$. In the same way, the other finite singular points can be determined from this spectrum, i.e., $(\lambda_{03}, \omega_{03})$, $(\lambda_{04}, \omega_{04})$, and so on. We can refer to the singular point of the beginning as the bifurcation parameter. In the same manner, the third and higher order parameters can be determined. The values of these parameters are listed in Table III. By undergoing all bifurcation points, the system will become a completely unstable situation, just like the double bifurcation and multiple bifurcation in some one-dimensional systems (e.g., in the simplex logistic equation), or it means that the chaos of a brown tide will happen. Finally, it reveals that the first critical point (λ_{01}) is a possible parameter in the outbreak of brown tide.

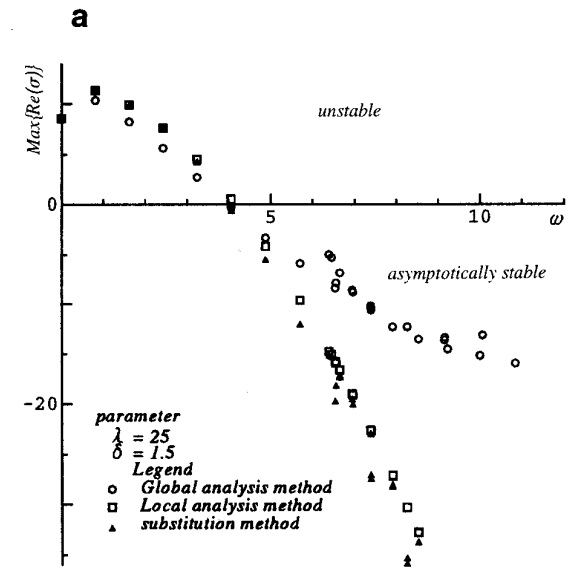

FIG. 4. Comparison of stability using three methods: (a) *Tubularia*; (b) brown tide.

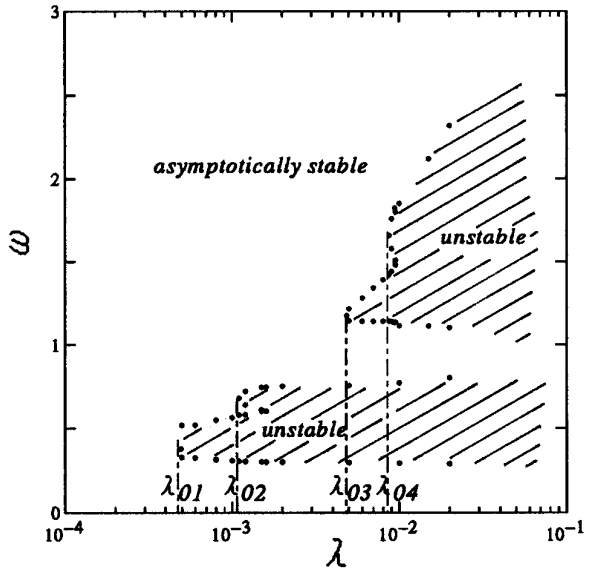

FIG. 5. Bifurcation diagram.

6.2.4. *Distribution of Phytoplankton from Linear Analysis*

Moreover, if we consider eigenvectors u_i as a base set in this linearized system, the possible solution u for system (2) can be approximated linearly, i.e.,

$$u = \Sigma a_i u_i, \quad i = 1, n, \tag{36}$$

where a_i are a set of the generalized coordinates and imply the oscillation amplitude for each wave number. As a result, a series of the combinations are shown on the right side of Fig. 6. These solutions represent the density distribution of phytoplankton in the brown tide on Sept. 17–23, 1978, respectively. The solutions are in good agreement with the observation shown in the left side of the same picture. In addition, by means of a trial and error method for the sake of simplicity, a set of a_i was obtained and listed in Table IV, we can find out that the eigenvectors with the larger number represent the perturbation oscillation in a higher wave number.

6.3. Stability of General Solutions for a Brown Tide

To investigate the stability and the solution period in reality, the solution which represents the distribution of phytoplankton in a brown tide on Sept. 17–23, 1978 is subject to verification as to its stability. In practice, a spatial solution has a periodic characteristic when time extends to infinity. In this section, it will be shown to be not only stable but periodic as well.

Each pattern of the general solution (from linear analysis as shown in Fig. 6 in the above section) is temporarily considered as a stationary state. By employing the finite

TABLE III

Bifurcation Parameters in the Brown Tide

No.	1	2	3	4
$\lambda_{0i} \times 10^{-3}$	0.495	1.100	4.850	8.700
ω_{0i}	0.377	0.665	1.190	1.660

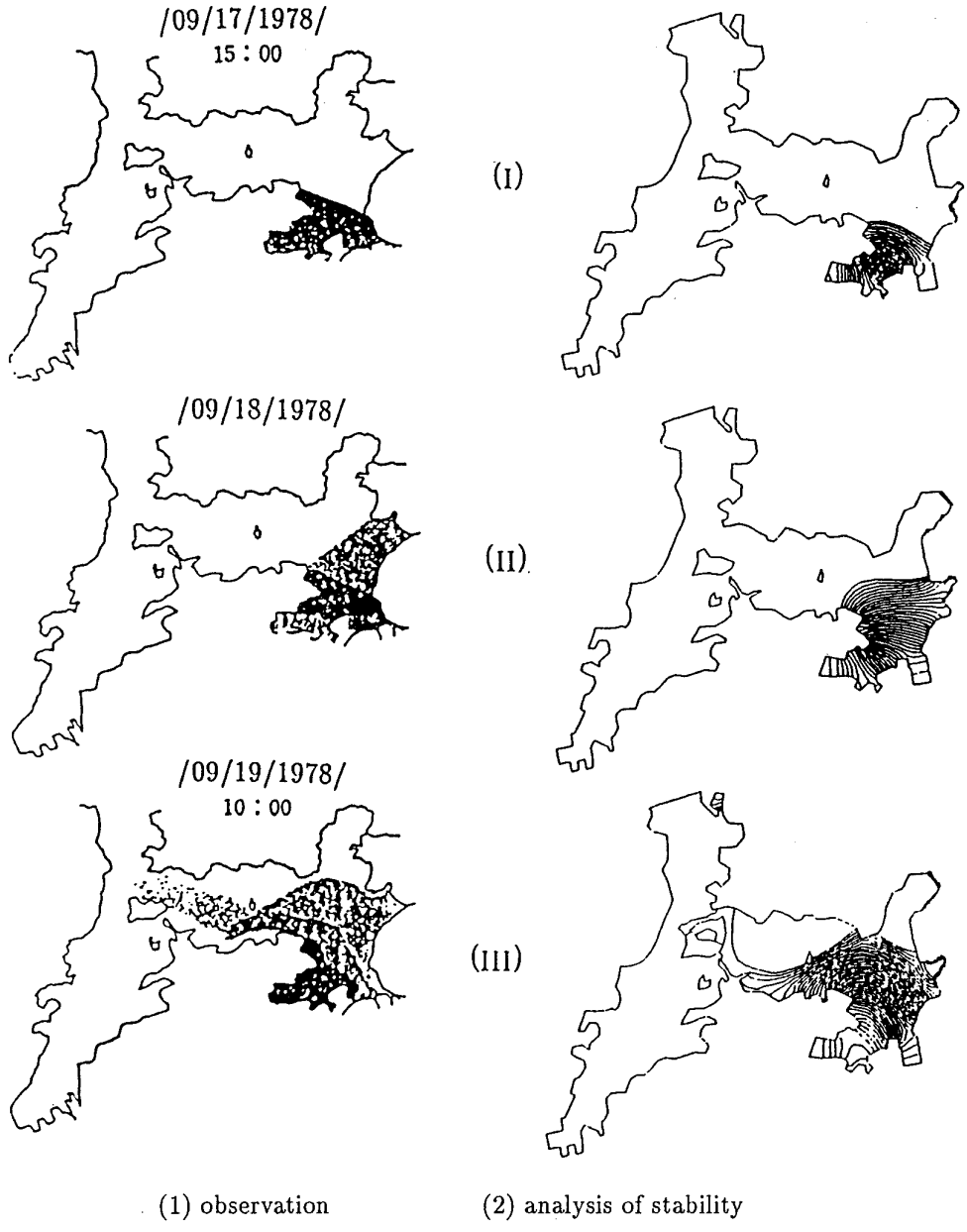

FIG. 6. Comparison of distribution of phytoplankton in brown tide.

element method (i.e., eigenvalue method) as described above and by taking the parameter $\lambda = 1.5 \times 10^{-3}$ close to the critical bifurcation parameter, the eigenspectrum for each pattern was computed to determine the stability of the stationary solution. Figure 7 illustrates the distribution of eigenvalues for all patterns in a complex plane. One can extract the maximum real part of each eigenspectrum for the above solution. Figure 8 can be obtained which shows all of the maximum real parts for each stationary solution and implies that the solutions are stable under Lyapunov's definition of stability. In Fig. 7, one can determine conjugate pairs of eigenvalues that cross the imaginary axis approximately, i.e.,

$$\sigma = \xi \pm i\eta, \tag{37}$$

where the real part ξ is very small and is close to zero, a general solution with perturbation can be represented as

$$\begin{aligned}\mathbf{u}(x, y, t) = \mathbf{u}_0(x, y) \\ + \Sigma\{\Phi_i(x, y)e^{(\xi_i + i\eta_i)t} + \overline{\Phi}_i(x, y)e^{(\xi_i - i\eta_i)t}\},\end{aligned} \tag{38}$$

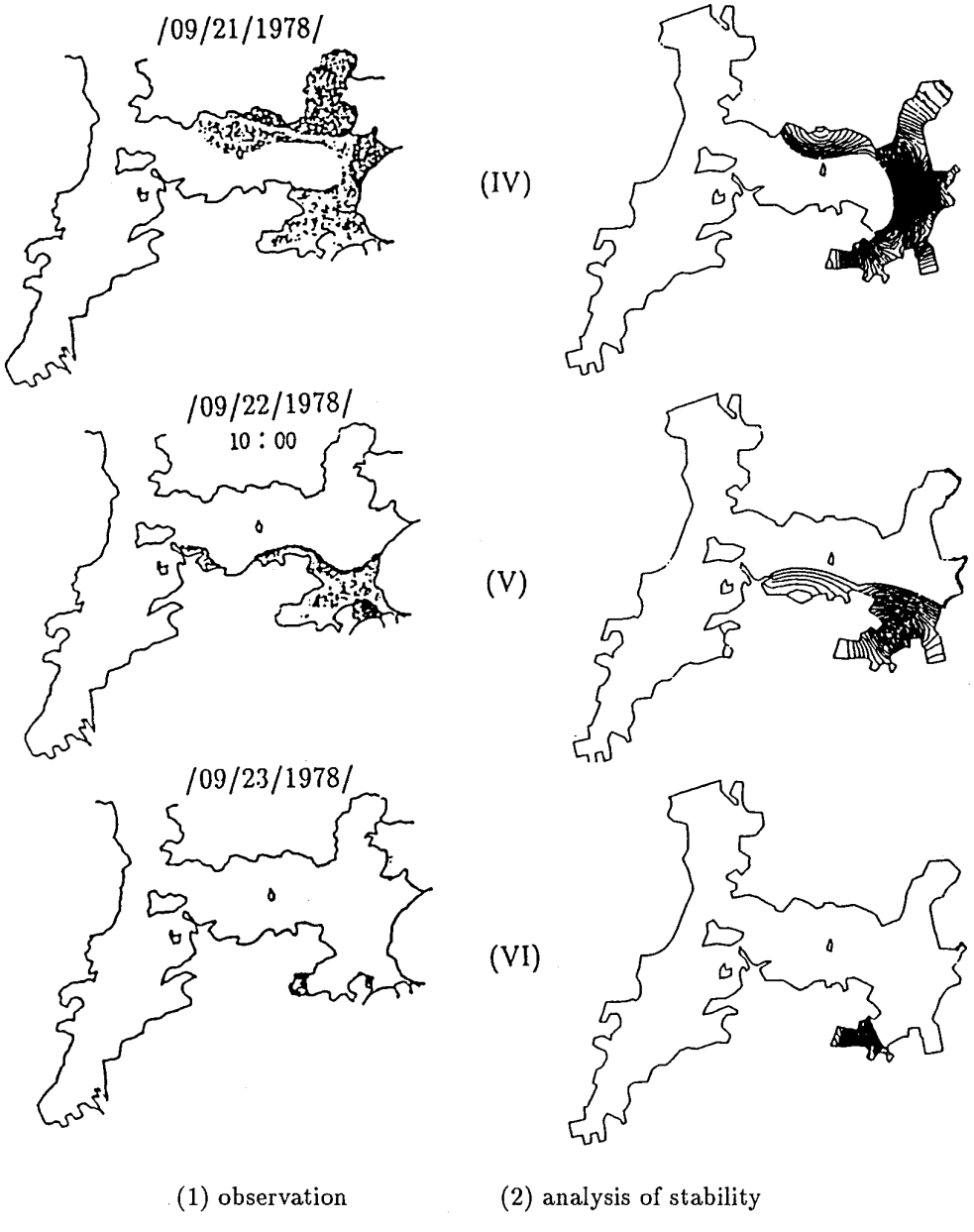

FIG. 6—*Continued*

TABLE IV

The Coordinates in the Base of the System

u	1	2	5	6	7	8	10	11	12	15	17	18
I	0	−0.2	−0.4	−0.2	0.1	−0.3	0	0	0	0	0	0
II	0	−0.39	−0.6	−0.33	0	0	0	0	0	0	0	0
III	0	−1.0	−0.8	−0.5	0	0	0	0	0	0	−0.45	0
IV	0.3	−1.0	−0.5	0.5	0	0	0	0	0	0	0.5	0
V	0	−0.06	−0.43	−0.4	0	−0.15	0	0	0	−0.11	−0.05	−0.025
VI	2.1	0	0	0	0	−0.6	0.6	−0.6	0.6	0	0	−0.12

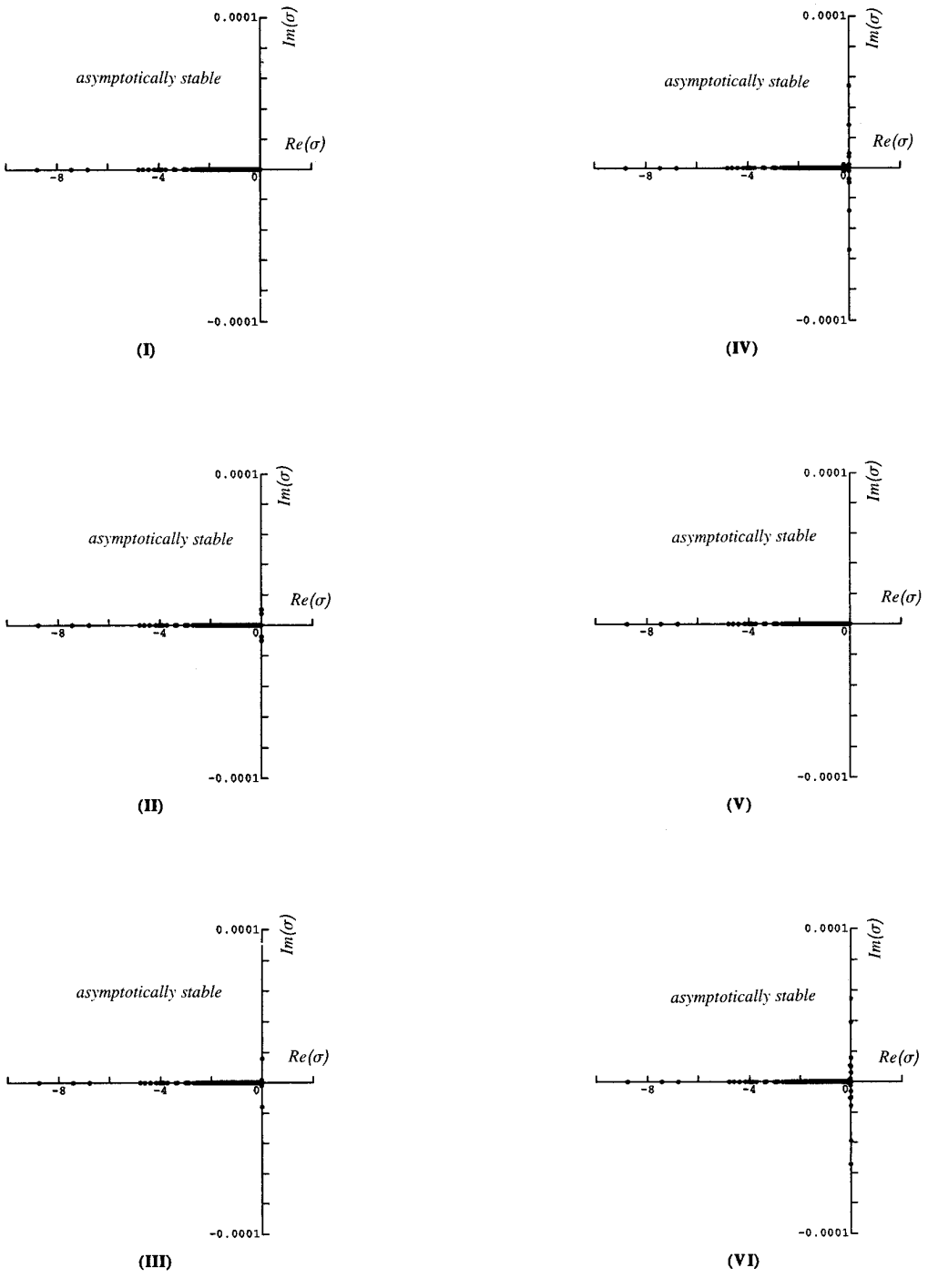

FIG. 7. Distribution of eigenvalues for each pattern in brown tide.

where Φ and $\overline{\Phi}$ denote the eigenvector and conjugate eigenvector, respectively. $\mathbf{u}_0$ is the stationary solution as shown in Fig. 6. Since the real part ξ is small enough in practical numerical calculation, $e^{\xi} \approx 1.0$. Meanwhile, as the imaginary part $e^{-i\eta}$ indicates the part of the periodic oscillation in a brown tide, several kinds of frequencies exist in the general solution. In Table V, both the frequencies and the period are listed in which the period is transformed into a practical one in terms of multiplication by time scale T_0. In general, the longest period of oscillation is close to 10 centuries in pattern (III) and the shortest one is about 33 years in pattern (IV). A frequency doubling

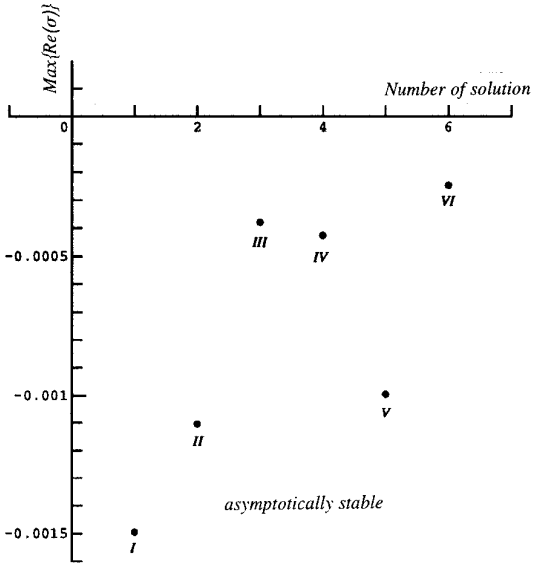

FIG. 8. Maximum real part of eigenvalues for each pattern.

relation also remains in the table as well. Those frequencies can be considered qualitatively as an explanation of the practical period in a brown tide with a large time scale.

7. CONCLUSION

In this paper, we analyzed the bifurcation of both *Tubularia* in a hollow cylinder and in a brown tide in Maizuru Harbor by means of the finite element method. Our conclusions are remarkable:

TABLE V

Frequency Spectrum for a General Solution in a Brown Tide

No.	Im(σ)	Frequency	Period (years)
II	1.02065E-05	1.62441E-06	175.68625
	7.47181E-06	1.18917E-06	239.98809
III	1.59071E-05	2.53170E-06	112.72551
	1.94154E-06	3.09007E-07	923.56475
IV	5.43078E-05	8.64336E-06	33.01818
	2.85316E-05	4.54096E-06	62.84753
	9.55573E-06	1.52084E-06	187.65137
	7.35011E-06	1.16980E-06	243.96172
	2.10721E-06	3.35373E-07	850.95726
VI	5.43519E-05	8.65038E-06	32.99138
	3.88927E-05	6.18997E-06	46.10489
	1.57165E-05	2.50137E-06	114.09258
	1.06979E-05	1.70263E-06	167.61515
	1.01980E-05	1.62306E-06	175.83276
	6.12699E-06	9.75141E-07	292.66338
	2.20374E-06	3.50736E-07	813.68189

1. The reaction–diffusion system can describe the growth of species in the *Tubularia* and the evolution of a brown tide. The homogeneous transportation of phytoplankton can be represented by a diffusion term and production is given by the reaction term.

2. The eigenvectors of the Helmholtz equation express the oscillation perturbation spectrum in the patch of hydranth regeneration in *Tubularia* and in a brown tide.

3. The most unstable eigenvector occurs in the smaller modes of the eigenvalue in the spectrum. It follows that there is a very unstable point in the system.

4. The combination of eigenvectors can be similar to the distribution of the patches in both *Tubularia* and the brown tide.

5. It is simple and effective to use spectrum analysis and substitution methods in order to check the stability of a linear system.

6. In particular, as regards the evolution of the brown tide (from the linearized point of view), we can consider the first singular point as the possible value in the onset of the brown tide. From the bifurcation diagram, by undergoing finite times bifurcation the system of reaction–diffusion will convert itself so as to be completely unstable.

By checking the stability of the spectrum, the bifurcation parameter λ is obtainable. This implies the onset of a brown tide in a parameter level. Meanwhile, by means of calculating eigenvalues, the frequency and the period for a brown tide can also be determined from the stationary solution which represents the distribution of phytoplankton in a brown tide that has periodic characteristics.

However, since an exponential function is provided for the reaction term, it is plausible to describe the reaction mechanism in a species of brown tide. Actually, a practical process presents the phenomena of both periodic and decay. In order to simulate the process more accurately, it is necessary to modify the reaction term in this model. In addition, it is important for the stability analysis to take the convective term (i.e., tidal flow) into account; however, doing so makes bifurcation analysis very complicated. Finally, although the problem of analysis in three-dimensional space is extremely complicated, it is possible and necessary to research the impact of waves in shallow water further in the assumption of well mixing in a vertical direction in the future. Moreover, in the period analysis for the general solution, the exact algorithm needed to extract the eigenvalue must be considered so as to determine the features of Hopf bifurcation.

REFERENCES

1. R. Aris, *The Mathematical Theory of Diffusion and Reaction in Permeable Catalysts, Vols. I, II* (*Oxford Univ. Press, Clarendon, London, 1975*).

2. N. F. Britton, G. Joly, and M.-C. Duban, *Bull. Math. Biol.* **45,** 311 (1983).
3. N. F. Britton, *Reaction–Diffusion Equations and Their Application to Biology* (Academic Press, London, 1986), p. 109.
4. H. Kielhöfer, *J. Differential Equations* **47,** 378 (1976).
5. A. R. Gourlay and G. A. Watson, *Computational Methods for Matrix Eigenproblems* (Wiley, New York, 1973), p. 123.
6. J. D. Murray, *Lecture on Nonlinear Differential Equation Models in Biology* (Oxford Univ. Press, Clarendon, London, 1977).
7. W. Sakamoto, *Physical Accumulation on Plankton in Brown Tide, Brown Tide-Mechanism of Onset and Strategies,* edited by Japan Society of Marine Product (Kouseisya Kouseikakukan Press, 1981). [Japanese]
8. L. V. Kantorovich and G. P. Akilov, *Functional Analysis,* 2nd ed. (Pergamon, Elmsford, NY, 1982), p. 258.
9. R. H. Gallagher, Finite-element method for instability analysis, in *Finite Element Handbook,* edited by H. Kardestuncer and D. H. Norrie (McGraw–Hill, New York, 1987), p. 249.
10. R. W. Clough and J. Penzien, Dynamics of Structure, 2nd ed. (McGraw–Hill, New York, 1993), p. 201.